RAPID COMMUNICATION

Effects of Li^+ on photoluminescence of Sr_3SiO_5: Sm^{3+} red phosphor*

Zhang Xin(张 新), Xu Xu-Hui(徐旭辉), Qiu Jian-Bei(邱建备), and Yu Xue(余 雪)†

College of Materials Science and Engineering, Kunming University of Science and Technology, Kunming 650093, *China*

(Received 18 March 2013; revised manuscript received 8 April 2013)

The structure and photoluminescence (PL) properties of Sr_3SiO_5: Sm^{3+} and Li^+-doped Sr_3SiO_5: Sm^{3+} red-emitting phosphors were investigated. Samples were prepared by the high-temperature solid-state method. PL spectra show that the concentration quenching occurs when the Sm^{3+} concentration is beyond 1.3 mol% in Sr_3SiO_5: Sm^{3+} phosphor without doping Li^+ ions. The concentration-quenching mechanism can be explained by the electric dipole–dipole interaction of Sm^{3+} ions. The incorporation of Li^+ ions into Sr_3SiO_5: Sm^{3+} phosphors, as a charge compensator, improves the PL properties. The lithium ions also suppress the concentration quenching in Sm^{3+} with concentration increased from 1.3 mol% to 1.7 mol%.

Keywords: photoluminescence, concentration quenching, charge compensation

PACS: 78.55.–m, 42.70.–a **DOI:** 10.1088/1674-1056/22/9/097801

1. Introduction

In the past few decades, much attention has been paid to white light-emitting diodes (LEDs).[1] Semiconductor white light-emitting diodes (WLEDs) have emerged as the fourth generation of illumination technology, and are expected to replace the traditional incandescent, fluorescent, and high intensity discharge lamps due to advantages such as energy-saving, long service life, low voltage, high efficiency, good stability, and adjustable color.[2,3] At present, commercial WLEDs are mainly realized by combining a GaN-based blue LED chip with $Y_3Al_5O_{12}$: Ce^{3+} (YAG: Ce) yellow phosphor.[4] However, this approach has several disadvantages, such as the halo effect of blue/yellow color separation and the poor color rendering caused by the absence of a red component in the spectrum. One solution to these problems is using near-ultraviolet (NUV) LED chip-excited tricolor phosphors to obtain the required color rendering properties.[1,5] However, this requires high-performance blue, green, and red phosphors that can be excited by UV light, so nowadays attention has turned to the fabrication of blue, green, and red phosphors that are highly efficient, highly stable in chemical, and low thermal quenching.[6,7] The current commercial red phosphor for UV LEDs is Y_2O_2S: Eu^{3+}. However, it is chemically unstable due to its sulfide nature, and it is uneconomical to use rare earth oxides. A red phosphor with high absorption in the near-UV/blue spectral region, that also offers chemical stability and low cost, is urgently needed for UV LEDs.[8–13]

Compared with sulfide-based phosphors, silicate-based phosphors have been found to be more chemically and thermally stable, and lower in cost. Therefore, in recent years silicate-based luminescent materials have become a research hotspot, and many studies on phosphors with a silicate as the host have been conducted.[14–17] Most researchers focus their attention on Eu^{2+} and Eu^{3+} ions as the luminescence center in red-emitting phosphors;[18–21] however, there are no papers that are devoted to the luminescence properties of Sm^{3+} ions as the luminescence center in red emission under NUV irradiation from Sr_3SiO_5. Sm^{3+} is a very effective activator, and its excitation and emission occur through a 4f–4f electric dipole transition.[22,23] Therefore, the combination has great potential for designing novel optical functional materials. As a charge compensator, Li^+ ions are incorporated into the host lattice of the phosphor.

In the present work, we develop a novel, stable red phosphor of Sr_3SiO_5: Sm^{3+}, Li^+ that can be excited effectively by NUV excitation. To the best of our knowledge, no novel red phosphor of Sr_3SiO_5: Sm^{3+}, Li^+ has been reported.

In this paper, we report the synthesis of the Sr_3SiO_5: Sm^{3+} and Li^+-doped Sr_3SiO_5: Sm^{3+} phosphors by using the high-temperature solid-state method. Li^+ acts as a charge compensator and is responsible for the improved photoluminescence (PL) properties. Sm^{3+} and Li^+ dopant concentrations are optimized in order to explore an excellent red phosphor. The enhanced PL intensity, improved crystallinity, and changed concentration-quenching behavior are discussed in detail.

2. Experiment

A series of Sr_3SiO_5: Sm^{3+} and Li^+-doped Sr_3SiO_5: Sm^{3+} phosphors with different activator concentrations were

*Project supported by the National Natural Science Foundation of China (Grant No. 11204113), the Specialized Research Fund for the Doctoral Program of Higher Education of China (Grant No. 20115314120001), the China Postdoctoral Science Foundation (Grant No. 2011M501424), and the Natural Science Foundation of Yunnan Province, China (Grant No. 2011FB022).

†Corresponding author. E-mail: yuyu6593@126.com

synthesized by the high-temperature solid-state method. The typical synthesis procedure is as follows. $SrCO_3$ (Aldrich, 99.9%), SiO_2 (Aldrich, 99.9%), NH_4F (Aldrich, 99.9%), Li_2CO_3 (Aldrich, 99.9%), and Sm_2O_3 (Aldrich, 99.995%) were used as the starting materials, and they were mixed and ground according to the appropriate stoichiometric ratio. After all the materials were ground thoroughly in an agate mortar, most of the mixture was made into tablets at the pressure of 3 MPa. The tablets were placed into an alumina crucible, in which a layer of the mixture was spread in the bottom and was sintered at 1400 °C for 4 h in an atmosphere of N_2/H_2 (N_2: 95%, H_2: 5%). In order to obtain pure Sr_3SiO_5 main phase and prevent the generation of the impure phase of Sr_2SiO_4, a reducing atmosphere was used in the sample preparation process. In some cases, as a charge compensator, Li_2CO_3 was added with a suitable concentration.

The phases of samples were identified by X-ray powder diffraction (XRD) with Ni-filtered Cu $K\alpha$ radiation ($\lambda = 0.15406$ nm) at a scanning step of 0.02. The XRD data were collected in the range of $10^\circ < 2\theta < 80^\circ$ by using a D8 ADVANCE/Germany Bruker X-ray diffractometer. A Hitachi F-7000 fluorescence spectrophotometer was used to record the excitation and emission spectra. The powder samples were compacted and excited under 45° incidence, and the emitted fluorescence was detected perpendicular to the excitation beam. The tablets were made by using a 769YP-24B powder compressing machine. All of the measurements were performed at room temperature.

3. Results and discussion

3.1. Composition and structure analysis

The XRD patterns of the Sr_3SiO_5, $Sr_{2.987}SiO_5$: $0.013Sm^{3+}$, and $Sr_{2.974}SiO_5$: $0.013Sm^{3+}$, $0.013Li^+$ phosphors are shown in Fig. 1. All diffraction peaks in the pattern agree with the standard card (JCPDS 26-0984), indicating that the crystal phase is Sr_3SiO_5. No impurity peaks are detected in any of the compositions, the result clearly suggests that Sm^{3+} and Li^+ have been incorporated into the lattice and hardly change the lattice structure. As reported in JCPDS 26-0984, the Sr_3SiO_5 compound has a tetragonal structure belonging to the space group $P4/ncc$. In the Sr_3SiO_5 structure, all O^{2-} ions are surrounded by regular octahedra of Sr^{2+} ions and the difference between them lies in the way in which these units are linked to each other and to the SiO_4^{4-} tetrahedra. Each Sr^{2+} ion is bonded to two oxygen atoms, and these two oxygen atoms have only one Sr^{2+} ion.[5] The crystal structure of Sr_3SiO_5 is shown in Fig. 2. Furthermore, the lattice parameters of the Sr_3SiO_5, $Sr_{2.987}SiO_5$: $0.013Sm^{3+}$, and $Sr_{2.974}SiO_5$: $0.013Sm^{3+}$, $0.013Li^+$ samples are calculated by the Unit Cell program in the tetragonal system based on the given XRD data (Fig. 1), as shown in Table 1. We can also find that the diffraction peaks of the Sr_3SiO_5, $Sr_{2.987}SiO_5$: $0.013Sm^{3+}$ and $Sr_{2.974}SiO_5$: $0.013Sm^{3+}$, $0.013Li^+$ samples shift slightly toward to the larger 2θ diffraction direction. This should be ascribed to the successful introduction of Sm^{3+} (95.8 pm) and/or Li^+ (76 pm) ions into the Sr^{2+} (118 pm) sites in the Sr_3SiO_5 structure, which leads to the slight contraction of the lattice volume in turn. In addition, the strong and sharp diffraction peaks indicate that these phosphors are highly crystallized, which may be advantageous to luminescence.

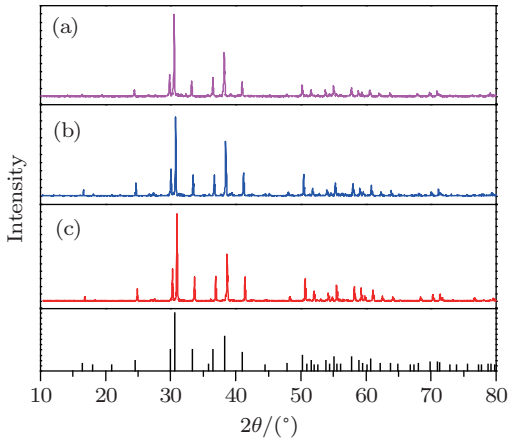

Fig. 1. XRD patterns of samples (a) Sr_3SiO_5, (b) $Sr_{2.987}SiO_5$:$0.013Sm^{3+}$, and (c) $Sr_{2.974}SiO_5$: $0.013Sm^{3+}$, $0.013Li^+$. The standard data for Sr_3SiO_5 (JCPDS 26-0984) is shown as a reference.

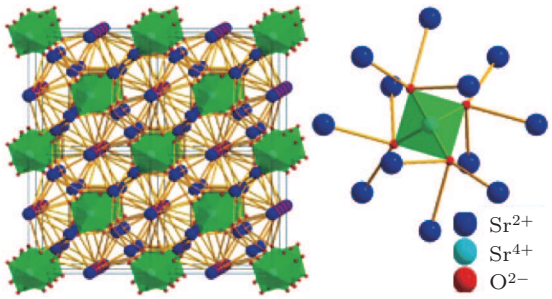

Fig. 2. The crystal structure of Sr_3SiO_5 phosphor.

Table 1. Change of the cell parameters of samples.

Phosphors	2θ (202)/(°)	$a = b$/Å	c/Å	V/Å^3
Sr_3SiO_5 (JCPDS26-0984)	30.601	6.948	10.753	519.0
Sr_3SiO_5 (this work)	30.940	6.956	10.760	520.6
$Sr_{2.987}SiO_5$: $0.013Sm^{3+}$	30.959	6.951	10.758	519.8
$Sr_{2.974}SiO_5$: $0.013Sm^{3+}$, $0.013Li^+$	30.978	6.932	10.778	517.9

3.2. Effect of Li^+ on PL intensity

The effect of the Sm^{3+} doping concentration on the emission spectrum and PL intensity of the $Sr_{3-x}SiO_5$: xSm^{3+} phosphor is investigated in detail, as shown in Fig. 3(a). It can be seen from the emission spectrum excited at 251 nm that several peaks in the red-orange area are located at 576 nm, 607 nm, and 655 nm, which are attributed to the typical $^4G_{5/2} \rightarrow {}^6H_{5/2}$, $^4G_{5/2} \rightarrow {}^6H_{7/2,}$ and $^4G_{5/2} \rightarrow {}^6H_{9/2}$ transitions of Sm^{3+} ions, respectively, and the strongest emission peak is located at 607 nm.[3]

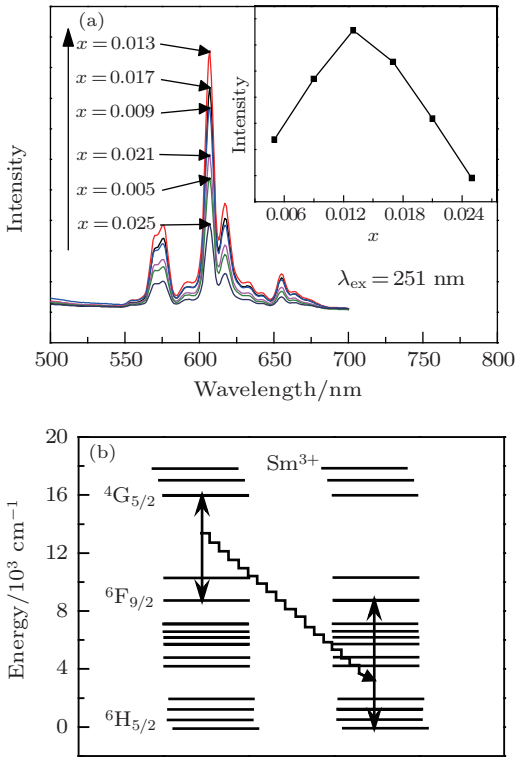

Fig. 3. (a) Emission intensity of the $Sr_{3-x}SiO_5$: xSm^{3+} phosphor with different Sm^{3+} concentration. The inset shows the relative PL intensity as a function of x at $\lambda_{ex} = 251$ nm. (b) Cross relaxation process diagram of Sm^{3+} ions.

As shown in the inset of Fig. 3(a), at low Sm^{3+} concentrations, the emission intensity increases with the increase of the Sm^{3+} concentration, and reaches the maximum when the concentration of Sm^{3+} is 1.3 mol%. Concentration quenching occurs when the Sm^{3+} concentration is beyond 1.3 mol%. As the concentration increases, the distance between Sm^{3+} ions becomes smaller, leading to a higher probability of energy transfer among Sm^{3+} ions. The concentration quenching of Sm^{3+} ions is mainly caused by the cross relaxation between the energy level couple $^4G_{5/2}-{}^6F_{9/2}$ and $^6H_{5/2}-{}^6F_{9/2}$, and the cross relaxation process is shown in Fig. 3(b). A rough estimation of the critical distance (R_c) for energy transfer can be made by using Blasse's formula[24,25]

$$R_c = 2\left(\frac{3V}{4\pi x_c N}\right)^{1/3}, \quad (1)$$

where V is the volume of the unit cell, x_c is the critical concentration of the activator ion, and N is the number of formula units per unit cell. In this case, $N = 4$, x_c and V are approximately taken as 1.3 mol% and 519.8 Å^3, respectively. Therefore, the critical distance of Sm^{3+} in Sr_3SiO_5, R_c, is estimated to be 2.67 nm.

The dependence of the integrated emission intensity at 607 nm under the 251 nm excitation on the concentration of the charge compensation of Li^+ is shown in Fig. 4. In order to investigate the effect of Li^+, the concentration of Sm^{3+} is fixed at 1.3 mol% and the concentration of Li^+ is changed from 0.5 mol% to 2.1 mol%. As the doping concentration of Li^+ increases, the red-emission intensity from Sm^{3+} increases until reaching a maximum when the concentration of Li^+ is equal to that of Sm^{3+} (1.3 mol%).

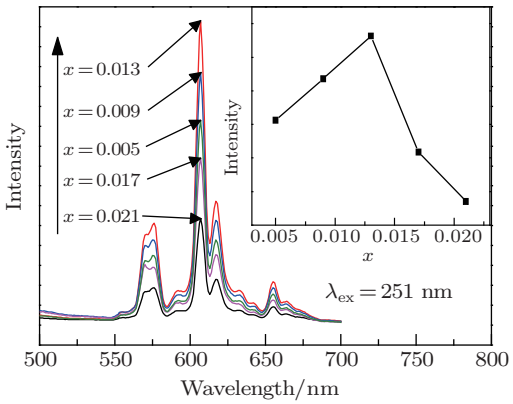

Fig. 4. The emission intensity of $Sr_{2.987-x}SiO_5$: $0.013Sm^{3+}$, xLi^+ phosphor with different Li^+ concentration, the inset shows the relative PL intensity as a function of x at $\lambda_{ex} = 251$ nm.

In $Sr_{3-x}SiO_5$: xSm^{3+}, trivalent Sm^{3+} ions not only play the role of activator, but also act as an aliovalent auxiliary dopant to create defects. When trivalent Sm^{3+} is doped into the Sr_3SiO_5 host lattice, Sm^{3+} substitutes chemically, but nonequivalently, in the Sr^{2+} sites. Due to these nonequivalent substitutions, an excess of positive charge in the lattice must be compensated to maintain the electroneutrality of these phosphors. There are two possible ways to realize the charge compensation. One possible way is that two Sm^{3+} ions substitute for three Sr^{2+} ions ($2Sm^{3+} + 3Sr^{2+} \rightarrow 2Sm^{\bullet}_{Sr} + V''_{Sr}$), which creates two positive defects of $Sm^{\bullet}_{Sr}$ and one vacancy defect of V''_{Sr} with two electrons ($V''_{Sr} \rightarrow V_{Sr} + 2e$). The other possible charge compensation is the vacancies of Sr^{2+}(V''_{Sr}) created during the synthesis process, which should be feasible because of the relatively high vapor pressure of the Sr^{2+} component.[26]

As a charge compensator, Li^+ ions can be introduced into the host lattice of Sr_3SiO_5: Sm^{3+} phosphor. The positive charge of Li^+ ions neutralizes the negative charge of V''_{Sr}, which reduces the defects of the phosphors. The PL intensity increases, reaching a maximum value when the concentration of Li^+ equals that of Sm^{3+}. A concentration of Li^+

higher or lower than that of Sm^{3+} is harmful to the PL intensity. Furthermore, phosphors doped with Li^+ ions have much better crystallinity than that of phosphors without Li^+ ions, as shown in Fig. 1. Therefore, the improvement of the crystallinity caused by Li^+ ions could be another reason for the improved PL performance.[27]

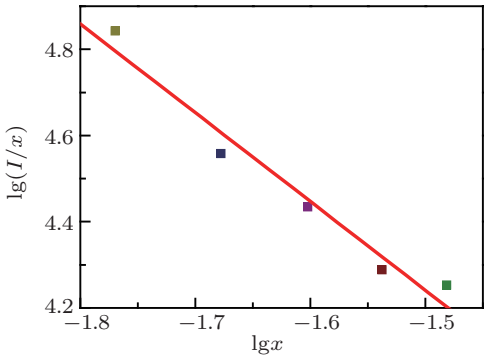

Fig. 5. The plot of $\lg(x) \sim \lg(I/x)$ in the selected $Sr_{3-2x}SiO_5$: xSm^{3+}, xLi^+ phosphor ($\lambda_{ex} = 251$ nm).

As discussed above, the concentration quenching is mainly caused by the nonradiative energy transfer among Sm^{3+} ions, which usually occurs as a result of an exchange interaction, radiation reabsorption, or an electric multipole-multipole interaction. Since the fluorescence mechanism of Sm^{3+} in Sr_3SiO_5: Sm^{3+}, Li^+ phosphor is the 4f–4f allowed electric-dipole transition, the process of energy transfer must be controlled by the electric multipole–multipole interaction. If the energy transfer occurs among the same sorts of activators, the intensity of the electric multipolar interaction can be determined from the change of the emission intensity from the emitting level that has the electric multipolar interaction. On the basis of the Dexter theory, the emission intensity per activator ion is given by the equation[28,29]

$$I/x = K[1+\beta(x)^{Q/3}]^{-1}, \tag{2}$$

where I is the emission intensity, x is the activator concentration; K and β are constants under the same excitation condition for a given host crystal; and $Q = 6$, 8, or 10 is for electric dipole–dipole (d–d), electric dipole–quadrupole (d–p), or electric quadrupole–quadrupole (q–q) interaction, respectively.

When x is higher than 1.3 mol%, we measure I at 607 nm, then draw the $\lg(x) \sim \lg(I/x)$ diagram of $Sr_{3-2x}SiO_5$: xSm^{3+}, xLi^+ ($x = 0.017$, 0.021, 0.025, 0.029, 0.033) phosphors, as shown in Fig. 5. It can be seen that the drawing is linear and the slope is -2.06. The Q value obtained is 6.18, which is approximately equal to 6. The consequence indicates that the electric dipole–dipole interaction is the major mechanism for the concentration quenching of the central Sm^{3+} emission in the Sm^{3+}-doped Sr_3SiO_5 phosphor.

3.3. Effect of Li^+ on concentration quenching

The diversification of the emission intensity (Sm^{3+} at 607 nm) of Sr_3SiO_5: Sm^{3+}, Li^+ as a function of the Sm^{3+} and Li^+ concentration under 251 nm excitation is shown in Fig. 6. The PL intensities of $Sr_{3-x}SiO_5$: xSm^{3+} and $Sr_{3-2x}SiO_5$: xSm^{3+}, xLi^+ under 251 nm excitation are displayed in Figs. 3(a) and 6, respectively. The intensity of the Sm^{3+} emission at 607 nm increases with increasing Sm^{3+} concentration, and then decreases when the concentration exceeds 1.3 mol% in $Sr_{3-x}SiO_5$: xSm^{3+}. In contrast with $Sr_{3-x}SiO_5$: xSm^{3+}, the concentration quenching is observed in $Sr_{3-2x}SiO_5$: xSm^{3+}, xLi^+ phosphors up to $x = 1.7$ mol%. As shown in the inset of each figure, the relative intensity is conspicuously enhanced by a factor of 2.2 in $Sr_{2.966}SiO_5$: $0.017Sm^{3+}$, $0.017Li^+$ compared to $Sr_{2.987}SiO_5$: $0.013Sm^{3+}$ phosphors. It is discovered that the doping of Li^+ into the Sr_3SiO_5: Sm^{3+} phosphor not only enhances PL, but also reduces the concentration-quenching effect.

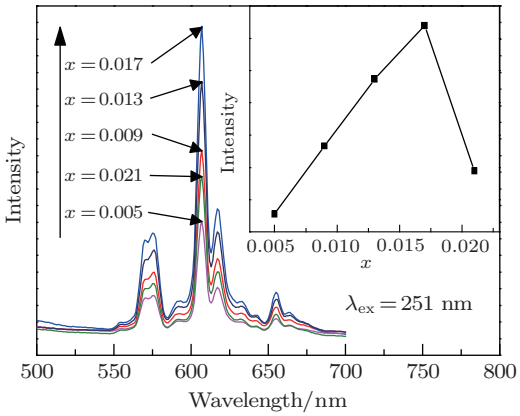

Fig. 6. Emission intensity of $Sr_{3-2x}SiO_5$: xSm^{3+}, xLi^+ phosphor with different Sm^{3+} and Li^+ concentrations, the inset shows the relative PL intensity as a function of x at $\lambda_{ex} = 251$ nm.

After doping with Li^+, a rough estimation of the critical distance (R_c) for energy transfer can be made using Blasse's formula (1). In this case, $N = 4$, x_c and V are approximately taken as 1.7 mol% and 516.7 Å^3, respectively. Therefore, the critical distance of Sm^{3+} in Sr_3SiO_5, is estimated to be 2.44 nm. This reveals the natural critical distance of Sm^{3+} in Sr_3SiO_5. It is concluded that Li^+ as a charge compensator reduces the defects in the Sr_3SiO_5: Sm^{3+} phosphor. With the elimination of defects in the host, the PL intensity is improved greatly.

4. Conclusion

In this work, Sr_3SiO_5: Sm^{3+} and Li^+-doped Sr_3SiO_5: Sm^{3+} red-emitting phosphors were prepared by using the high-temperature solid-state method. The effect of doping concentration of Sm^{3+} and Li^+ on the PL properties of the Sr_3SiO_5: Sm^{3+} phosphor was investigated in detail. The PL

spectra show that the concentration quenching occurs when the Sm^{3+} concentration is beyond 1.3 mol% in Sr_3SiO_5: Sm^{3+} phosphor without doping Li^+ ions. The concentration quenching of Sm^{3+} ions is mainly caused by the cross relaxation between the energy level couples $^4G_{5/2}-^6F_{9/2}$ and $^6H_{5/2}-^6F_{9/2}$. As a charge compensator, Li^+ ions were incorporated into Sr_3SiO_5: Sm^{3+} phosphors, which improves the PL properties. It is discovered that the doping of Li^+ into the Sr_3SiO_5: Sm^{3+} phosphor not only enhances PL, but also reduces the concentration-quenching effect. The concentration-quenching mechanism can be explained by the electric dipole–dipole interaction of the Sm^{3+} ions.

References

[1] Chen Y, Yang H K, Park S W, Moon B K, Choi B C, Jeong J H and Kim K H 2012 *J. Alloys Compd.* **511** 123

[2] Zhou T L, Song Z, Song X P, Bian L and Liu Q L 2010 *Chin. Phys. B* **19** 127808

[3] Yang Z P, Wang S L, Yang G W, Tian J, Li P L and Li X 2007 *J. Chin. Ceramic Soc.* **35** 1587

[4] Guo N, Huang Y J, Yang M, Song Y H, Zheng Y H and You H P 2011 *Phys. Chem. Chem. Phys.* **13** 15077

[5] Shen C Y, Li K and Yang Y 2011 2009 *Asia-Pacific Optical Fiber Communication and Optoelectronic International Conference*, November 2–6, 2009, Shanghai, China, p. 7635

[6] Lakshmanan A, Bhaskar R S, Thomas P C, Kumar R S, Kumar V S and Jose M T 2010 *Mater. Lett.* **64** 1809

[7] Kim K, Moon Y M, Choi S, Jung H K and Nahm S 2008 *Mater. Lett.* **62** 3925

[8] Reddy K R, Annapurna K and Buddhudu S 1996 *Mater. Res. Bull.* **31** 1355

[9] Yuan S L, Yang Y X, Fang B and Chen G R 2007 *Opt. Mater.* **30** 535

[10] Xie A, Yuan X M, Wang F X, Shi Y and Mu Z F 2010 *J. Phys. D: Appl. Phys.* **43** 055101

[11] Zhang Y, Xu J Y and Zhang T T 2011 *J. Inorg. Mater.* **26** 1341

[12] Mu Z F, Hu Y H, Chen L and Wang X J 2011 *Opt. Mater.* **34** 89

[13] Sun J Y, Lai J L, Sun J F and Du H Y 2011 *J. Chin. Rare Earth Soc.* **24** 321

[14] Kim S H, Lee H J, Kim K P and Yoo J S 2006 *Korean J. Chem. Eng.* **23** 669

[15] Ji Z G, Zhao S C, Xiang Y, Song Y L and Ye Z Z 2004 *Chin. Phys.* **13** 0561

[16] Yu H, Deng D G, Li Y Q, Xu S Q, Li Y Y, Yu C P, Ding Y Y, Lu H W, Yin H Y and Nie Q L 2013 *Opt. Commun.* **289** 103

[17] Cheng G, Liu Q S, Cheng L Q, Lu L P, Sun H Y, Wu Y Q, Bai Z H, Zhang X Y and Qiu G M 2010 *J. Chin. Rare Earth Soc.* **28** 526

[18] Zhang J C, Zhou M J and Wang Y 2012 *Chin. Phys. B* **21** 124102

[19] Wang Z J, Li P L, Yang Z P, Guo Q L and Li X 2010 *Chin. Phys. B* **19** 017801

[20] Wei X D, Cai L Y, Lu F C, Chen X L, Chen X Y and Liu Q L 2009 *Chin. Phys. B* **18** 3555

[21] Huang P, Cui C E and Wang S 2009 *Chin. Phys. B* **18** 4524

[22] Jayasankar C K and Babu P 2000 *J. Alloys Compd.* **307** 82

[23] Yang D L, Lin H, Hou Y Y, Xu L Q, Zhai B, Ban L X, Liu G S, Tang N L, Wang S C, Ma T C, Wang X J and Liu X R 2006 *Spectrosc. Spect. Anal.* **26** 86

[24] Xia Z G and Liu R S 2012 *J. Phys. Chem. C* **116** 15604

[25] Blasse G 1968 *Phys. Lett. A* **28** 444

[26] Liu Y L, Kuang J Y, Lei B F and Shi C S 2005 *J. Mater. Chem.* **15** 4025

[27] Liao N, Shi L Y, Jia H, Yu X J, Jin D L and Wang L C 2010 *Inorg. Mater.* **46** 1325

[28] Xie W, Wang Y H, Zou C W, Liang F, Quan J, Zhang J and Shao L 2013 *Chin. Phys. B* **22** 056101

[29] Luo H D, Liu J, Zheng X, Han L X, Ren K X and Yu X B 2012 *J. Mater. Chem.* **22** 15887